

SAM Struggles in Concealed Scenes – Empirical Study on “Segment Anything”

Ge-Peng Ji, Deng-Ping Fan, Peng Xu, Ming-Ming Cheng, Bowen Zhou, Luc Van Gool

Abstract—Segmenting anything is a ground-breaking step toward artificial general intelligence, and the Segment Anything Model (SAM) greatly fosters the foundation models for computer vision. We could not be more excited to probe the performance traits of SAM. In particular, exploring situations in which SAM does not perform well is interesting. In this report, we choose three concealed scenes, *i.e.*, camouflaged animals, industrial defects, and medical lesions, to evaluate SAM under unprompted settings. Our main observation is that SAM looks unskilled in concealed scenes.

Index Terms—Segment Anything, SAM, Camouflaged, Concealed Scene Understanding, Concealed Object Segmentation.

1 INTRODUCTION

LARGE models open up new opportunities for artificial intelligence. In the past few months, there has been a boom in training foundation models on the vast linguistic corpus to produce amazing applications, *e.g.*, ChatGPT¹, GPT-4². Both natural language processing and multimodal learning communities have been revolutionized. Large models’ capacity for generalization and emergent makes it easy for users to believe that large models can solve anything.

Last week, the “Segment Anything” [1] project was released, and its Segment Anything Model (SAM) is a large ViT-based model trained on the large visual corpus (SA-1B). This is a ground-breaking step toward artificial general intelligence, as SAM demonstrates promising segmentation capabilities in various scenarios and the great potential of the foundation models for computer vision. Like all computer vision researchers, we cannot wait to probe the performance traits of SAM to help the community to comprehend it further. Moreover, it is interesting to explore the situations in which SAM does not work well.

In this paper, we compare SAM quantitatively with cutting-edge models on camouflaged object segmentation task, and present diversified visualization results in three concealed scenes³ [2], *i.e.*, camouflaged animals, industrial defects, and medical lesions. Our main observation is that SAM looks not skillful in concealed scenes.

2 EXPERIMENT

We use three frequently-used camouflaged object segmentation (COS) benchmarks to evaluate SAM. Next, we describe our mask selection strategy (§2.1) and evaluation protocols (§2.2), compare

SAM with the state-of-the-art models of COS (§2.3), and provide qualitative visualisations on three concealed scenarios (§2.4).

2.1 Mask Selection Strategy

If under the unprompted setting, SAM generates multiple binary masks and can pop out several potential objects within an input. For a fair evaluation of interesting regions in a specific segmentation task, we take a strategy to select the most appropriate mask based on its ground-truth mask. Formally, given N binary predictions $\{\mathbf{P}_n\}_{n=1}^N$ and the ground-truth \mathbf{G} for an input image, we calculate intersection over union (IoU) scores for each pair to generate a set of evaluation scores $\{\text{IoU}_n\}_{n=1}^N$. We finally select the mask with the highest IoU score from this set.

2.2 Evaluation Protocols

Our protocols are following the standard practice as in [3].

• **Datasets.** We use three commonly-used COS benchmarks in our experiments, including CAMO [4] (250 samples), COD10K [5] (2,026 samples), and NC4K [6] (4,121 samples).

• **Models.** To ensure a fair comparison with SAM, we choose the current top-performing COS models using transformer architecture, *i.e.*, CamoFormer-P/S [7], HitNet [8].

• **Metrics.** We use five commonly-used metrics for the evaluation: structure measure (S_α) [9], enhanced-alignment measure (E_ϕ) [10], F-measure (F_β) [11], [12], weighted F-measure (F_β^w) [13], and mean absolute error (M). According to different thresholding strategies, the adaptive/mean/maximum values of F-measure and E-measure are reported. We denote different E_ϕ scores as E_ϕ^{ad} , E_ϕ^{mn} , and E_ϕ^{mx} .

2.3 Quantitative Evaluation

We report the quantitative comparison in Table 1, SAM demonstrates significant improvements as model capabilities increase from ViT-B to ViT-L, with an increase in F_β^w score from 0.353 to 0.655 on CAMO. However, the improvement is limited when the model becomes larger, increasing only from 0.655 (ViT-L) to 0.700 (ViT-H). Moreover, we observe that there remains a large gap between SAM even with ViT-H and current top-performing COS models on three benchmarks. For example as presented in

- Ge-Peng Ji is with the College of Engineering, Computing & Cybernetics, ANU, Canberra, Australia.
- Deng-Ping Fan and Luc Van Gool are with the Computer Vision Lab (CVL), ETH Zurich, Zurich, Switzerland.
- Peng Xu and Bowen Zhou are with the Department of Electronic Engineering, Tsinghua University, Beijing, China.
- Ming-Ming Cheng is with the Nankai University, Tianjin, China.

1. <https://chat.openai.com>

2. <https://openai.com/research/gpt-4>

3. There is a newly released survey on deep concealed scene understanding [2] (Project link: <https://github.com/DengPingFan/CSU>).

TABLE 1

Quantitative comparison on three popular COS benchmarks. The symbols \uparrow/\downarrow indicate that a higher/lower score is better. The highest scores are marked in bold. Δ represents the difference between SAM and the highest score achieved by current cutting-edge COS models.

| | Model | Pub/Year | Backbone | $S_\alpha \uparrow$ | $F_\beta^w \uparrow$ | $M \downarrow$ | $E_\phi^{ad} \uparrow$ | $E_\phi^{mn} \uparrow$ | $E_\phi^{mx} \uparrow$ | $F_\beta^{ad} \uparrow$ | $F_\beta^{mn} \uparrow$ | $F_\beta^{mx} \uparrow$ |
|------------|------------------|---------------------|-------------------------|---------------------|----------------------|----------------|------------------------|------------------------|------------------------|-------------------------|-------------------------|-------------------------|
| COD10K [5] | CamoFormer-P [7] | arXiv ₂₃ | PVTv2-B4 [14] | 0.869 | 0.786 | 0.023 | 0.931 | 0.932 | 0.939 | 0.794 | 0.811 | 0.829 |
| | CamoFormer-S [7] | arXiv ₂₃ | Swin-B [15] | 0.862 | 0.772 | 0.024 | 0.932 | 0.931 | 0.941 | 0.780 | 0.799 | 0.818 |
| | HitNet [8] | AAAI ₂₃ | PVTv2-B2 [14] | 0.871 | 0.806 | 0.023 | 0.936 | 0.935 | 0.938 | 0.818 | 0.823 | 0.838 |
| | SAM [1] | arXiv ₂₃ | ViT-B [16] | 0.585 | 0.353 | 0.108 | 0.535 | 0.533 | 0.535 | 0.423 | 0.422 | 0.423 |
| | | | Difference (Δ) | -28.6% | -45.3% | +8.5% | -40.1% | -40.2% | -40.3% | -39.5% | -40.1% | -41.5% |
| | | | ViT-L [16] | 0.751 | 0.655 | 0.065 | 0.766 | 0.764 | 0.766 | 0.718 | 0.716 | 0.718 |
| | | | Difference (Δ) | -12% | -15.1% | +4.2% | -17% | -17.1% | -17.2% | -10% | -10.7% | -12% |
| | | | ViT-H [16] | 0.781 | 0.700 | 0.054 | 0.800 | 0.798 | 0.800 | 0.756 | 0.754 | 0.756 |
| | | | Difference (Δ) | -9% | -10.6% | +3.1% | -13.6% | -13.7% | -13.8% | -6.2% | -6.9% | -8.2% |
| | Model | Pub/Year | Backbone | $S_\alpha \uparrow$ | $F_\beta^w \uparrow$ | $M \downarrow$ | $E_\phi^{ad} \uparrow$ | $E_\phi^{mn} \uparrow$ | $E_\phi^{mx} \uparrow$ | $F_\beta^{ad} \uparrow$ | $F_\beta^{mn} \uparrow$ | $F_\beta^{mx} \uparrow$ |
| CAMO [4] | CamoFormer-P [7] | arXiv ₂₃ | PVTv2-B4 [14] | 0.872 | 0.831 | 0.046 | 0.931 | 0.929 | 0.938 | 0.853 | 0.854 | 0.868 |
| | CamoFormer-S [7] | arXiv ₂₃ | Swin-B [15] | 0.876 | 0.832 | 0.043 | 0.935 | 0.930 | 0.938 | 0.856 | 0.856 | 0.871 |
| | HitNet [8] | AAAI ₂₃ | PVTv2-B2 [14] | 0.849 | 0.809 | 0.055 | 0.910 | 0.906 | 0.910 | 0.833 | 0.831 | 0.838 |
| | SAM [1] | arXiv ₂₃ | ViT-B [16] | 0.462 | 0.238 | 0.219 | 0.402 | 0.401 | 0.402 | 0.312 | 0.312 | 0.312 |
| | | | Difference (Δ) | -41.4% | -59.4% | +17.6% | -53.3% | -52.9% | -53.6% | -54.4% | -54.4% | -55.9% |
| | | | ViT-L [16] | 0.630 | 0.534 | 0.162 | 0.628 | 0.626 | 0.628 | 0.617 | 0.615 | 0.617 |
| | | | Difference (Δ) | -24.6% | -29.8% | +11.9% | -30.7% | -30.4% | -31% | -23.9% | -24.1% | -25.4% |
| | | | ViT-H [16] | 0.677 | 0.594 | 0.136 | 0.682 | 0.680 | 0.682 | 0.670 | 0.668 | 0.670 |
| | | | Difference (Δ) | -19.9% | -23.8% | +9.3% | -25.3% | -25% | -25.6% | -18.6% | -18.8% | -20.1% |
| | Model | Pub/Year | Backbone | $S_\alpha \uparrow$ | $F_\beta^w \uparrow$ | $M \downarrow$ | $E_\phi^{ad} \uparrow$ | $E_\phi^{mn} \uparrow$ | $E_\phi^{mx} \uparrow$ | $F_\beta^{ad} \uparrow$ | $F_\beta^{mn} \uparrow$ | $F_\beta^{mx} \uparrow$ |
| NC4K [6] | CamoFormer-P [7] | arXiv ₂₃ | PVTv2-B4 [14] | 0.892 | 0.847 | 0.030 | 0.941 | 0.939 | 0.946 | 0.863 | 0.868 | 0.880 |
| | CamoFormer-S [7] | arXiv ₂₃ | Swin-B [15] | 0.888 | 0.840 | 0.031 | 0.941 | 0.937 | 0.946 | 0.857 | 0.863 | 0.877 |
| | HitNet [8] | AAAI ₂₃ | PVTv2-B2 [14] | 0.875 | 0.834 | 0.037 | 0.928 | 0.926 | 0.929 | 0.854 | 0.853 | 0.863 |
| | SAM [1] | arXiv ₂₃ | ViT-B [16] | 0.544 | 0.334 | 0.166 | 0.494 | 0.493 | 0.494 | 0.403 | 0.403 | 0.403 |
| | | | Difference (Δ) | -34.8% | -51.3% | +13.6% | -44.7% | -44.6% | -45.2% | -46% | -46.5% | -47.7% |
| | | | ViT-L [16] | 0.728 | 0.643 | 0.101 | 0.735 | 0.733 | 0.735 | 0.706 | 0.704 | 0.706 |
| | | | Difference (Δ) | -16.4% | -20.4% | +7.1% | -20.6% | -20.6% | -21.1% | -15.7% | -16.4% | -17.4% |
| | | | ViT-H [16] | 0.763 | 0.696 | 0.087 | 0.777 | 0.775 | 0.777 | 0.752 | 0.750 | 0.752 |
| | | | Difference (Δ) | -12.9% | -15.1% | +5.7% | -16.4% | -16.4% | -16.9% | -11.1% | -11.8% | -12.8% |



Fig. 1. SAM [1] fails to perceive the animals that are visually “hidden” in their natural surroundings. All the samples are from COD10K dataset [5].

Table 1, the difference of E_ϕ^{mx} score between SAM (ViT-H) and CamoFormer-S [7] reaches 13.8% on COD10K dataset, 25.6% on CAMO dataset, and 16.9% on NC4K dataset. This gap indicates that the perception ability of SAM needs further improvement for concealed scenes.

2.4 Qualitative Comparison

We further qualitatively evaluate SAM in three concealed scenarios, and several interesting findings are as follows. All the visualisation results are generated by the [online demo](#) of SAM. *a) Camouflaged animal.* As presented in Fig. 1, it is difficult for SAM to detect concealed animals in their natural habitat. SAM

fails to segment a mantis crouching on a leaf (in the second column) and a seahorse swimming in an orange coral (in the last column). In these two cases, SAM struggles to distinguish the target semantics from their surroundings because the foreground and background share similar appearances of shape and colour. As a result, SAM becomes more dependent on unreliable pixel intensity changes along the boundaries. *b) Industrial defect.* In this scenario, given a product, it is usually collected by the close-range shots, occupying a large area in the image, and SAM’s behaviour appears to segment the main part of the object, such as the screw in the 3rd column and bottle in the 5th column of Fig. 2. Furthermore, we notice that it is difficult for SAM to distinguish defective

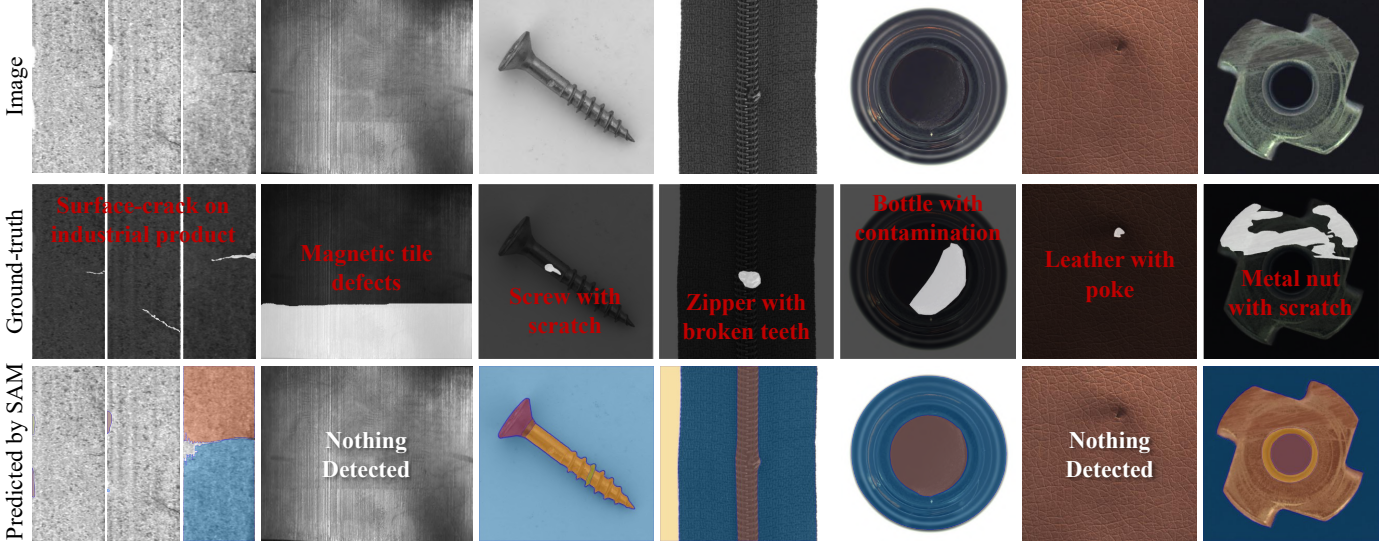


Fig. 2. SAM [1] is unskilled in detecting concealed defects in industrial scenes. These samples are taken from KolektorSDD [17], MagneticTile [18], and MVTECAD [19] datasets.

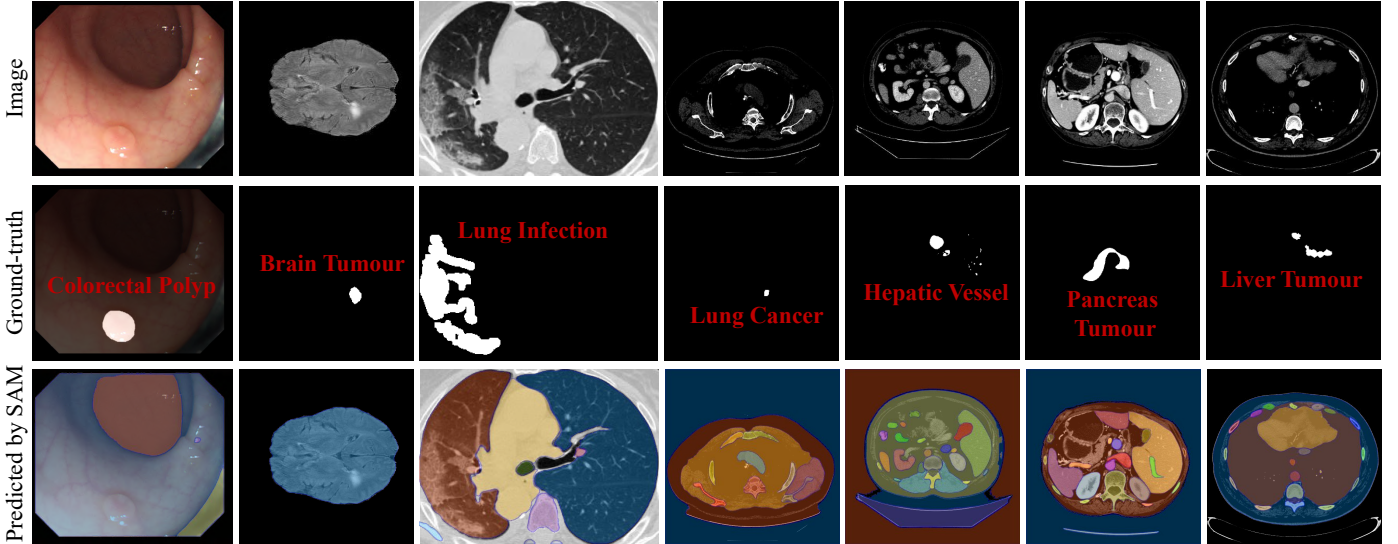


Fig. 3. SAM [1] fails to detect these lesion regions in various medical modalities. These samples cover the RGB colour modality from CVC-300 [20] (1st column); the MRI modality from BraTS2021 [21] (2nd column); the CT modalities from COVID-SemiSeg [22] (3rd column) and MSD [23] (from 4th to 7th columns).

areas from the textured background. For instance, products with surface cracks (in 1st column) and leather with a poke (in the 6th column) are challenging to identify accurately. This phenomenon is not surprising because SAM is trained on natural objects with standard sizes and high-contrast attributes. *c) Medical lesion.* As illustrated in 1st column of Fig. 3, we observe that SAM does not handle medical data with concealed patterns well, such as benign colorectal polyps that share similar colours with the surrounding tissues. The remaining samples in Fig. 3 are grayscale slices from three-dimensional MRI and CT scans. SAM can roughly segment the organ regions since they have distinct boundaries, but it does not perform well in recognizing amorphous lesion regions, *e.g.*, cancer, vessels, and tumours. This suggests that SAM lacks the medical domain knowledge of these anatomical and pathological cases. To alleviate this limitation, the intrinsic relationships and semantics of anatomical structures can be injected into SAM, such as the assumption that liver tumours should be inside the liver, rather than the brain.

2.5 Discussion

From the above empirical analyses, our conclusions are:

- We observe that SAM often segments an occluded object into multiple separated masks, indicating that its semantic capabilities in concealed scenes can be improved.
- Unlike self-supervised large language models, SAM employs supervised training, in our experiments its emergent and reasoning abilities have not been observed. Thus, it would be interesting to try if more challenging training tasks improve its performance.
- Considering the practical open-set problem, now the granularity and uncertainty are the bottlenecks of SAM, limiting its applications to the scenes that require high accuracy, *e.g.*, autonomous driving and clinical diagnosis. To alleviate this issue, one potential solution is to support the model with prior knowledge.
- SAM's great success is demonstrating the power of data-centric AI in the large model era. We see a significant trend that human feedback-based learning and large foundation models bring new opportunities for the vision community.

3 CONCLUSION

In summary, this paper presents an empirical study of SAM. Firstly, we quantitatively evaluate SAM using cutting-edge models on the camouflaged object segmentation task. Secondly, we present several failure cases in three concealed scenarios: camouflaged animals, industrial defects, and medical lesions. We expect that this paper helps the readers to comprehend SAM's performance traits in concealed scenes and brings new ideas to computer vision researchers.

REFERENCES

- [1] A. Kirillov, E. Mintun, N. Ravi, H. Mao, C. Rolland, L. Gustafson, T. Xiao, S. Whitehead, A. C. Berg, W.-Y. Lo *et al.*, "Segment anything," *arXiv preprint arXiv:2304.02643*, 2023.
- [2] D.-P. Fan, G.-P. Ji, P. Xu, M.-M. Cheng, C. Sakaridis, and L. Van Gool, "Advances in deep concealed scene understanding," *arXiv preprint arXiv:2304.11234*, 2023.
- [3] D.-P. Fan, G.-P. Ji, M.-M. Cheng, and L. Shao, "Concealed object detection," *IEEE Trans. Pattern Anal. Mach. Intell.*, vol. 44, no. 10, pp. 6024–6042, 2022.
- [4] T.-N. Le, T. V. Nguyen, Z. Nie, M.-T. Tran, and A. Sugimoto, "Anabranch network for camouflaged object segmentation," *Comput. Vis. Image Underst.*, vol. 184, pp. 45–56, 2019.
- [5] D.-P. Fan, G.-P. Ji, G. Sun, M.-M. Cheng, J. Shen, and L. Shao, "Camouflaged object detection," in *IEEE Conf. Comput. Vis. Pattern Recog.*, 2020, pp. 2777–2787.
- [6] Y. Lv, J. Zhang, Y. Dai, A. Li, B. Liu, N. Barnes, and D.-P. Fan, "Simultaneously localize, segment and rank the camouflaged objects," in *IEEE Conf. Comput. Vis. Pattern Recog.*, 2021, pp. 11 591–11 601.
- [7] B. Yin, X. Zhang, Q. Hou, B.-Y. Sun, D.-P. Fan, and L. Van Gool, "Camof-former: Masked separable attention for camouflaged object detection," *arXiv preprint arXiv:2212.06570*, 2023.
- [8] X. Hu, D.-P. Fan, X. Qin, H. Dai, W. Ren, Y. Tai, C. Wang, and L. Shao, "High-resolution iterative feedback network for camouflaged object detection," in *AAAI Conf. Art. Intell.*, 2023.
- [9] D.-P. Fan, M.-M. Cheng, Y. Liu, T. Li, and A. Borji, "Structure-measure: A new way to evaluate foreground maps," in *Int. Conf. Comput. Vis.*, 2017, pp. 4548–4557.
- [10] D.-P. Fan, G.-P. Ji, X. Qin, and M.-M. Cheng, "Cognitive vision inspired object segmentation metric and loss function," *SCIENTIA SINICA Informationis*, vol. 6, p. 6, 2021.
- [11] A. Borji, M.-M. Cheng, H. Jiang, and J. Li, "Salient object detection: A benchmark," *IEEE Trans. Image Process.*, vol. 24, no. 12, pp. 5706–5722, 2015.
- [12] M. Zhuge, D.-P. Fan, N. Liu, D. Zhang, D. Xu, and L. Shao, "Salient object detection via integrity learning," *IEEE Transactions on Pattern Analysis and Machine Intelligence*, 2022.
- [13] R. Margolin, L. Zelnik-Manor, and A. Tal, "How to evaluate foreground maps?" in *IEEE Conf. Comput. Vis. Pattern Recog.*, 2014, pp. 248–255.
- [14] W. Wang, E. Xie, X. Li, D.-P. Fan, K. Song, D. Liang, T. Lu, P. Luo, and L. Shao, "Pvt v2: Improved baselines with pyramid vision transformer," *Computational Visual Media*, vol. 8, no. 3, pp. 415–424, 2022.
- [15] Z. Liu, Y. Lin, Y. Cao, H. Hu, Y. Wei, Z. Zhang, S. Lin, and B. Guo, "Swin transformer: Hierarchical vision transformer using shifted windows," in *Proceedings of the IEEE/CVF international conference on computer vision*, 2021, pp. 10 012–10 022.
- [16] A. Kolesnikov, D. Weissenborn, X. Zhai, T. Unterthiner, M. Dehghani, M. Minderer, G. Heigold, S. Gelly, J. Uszkoreit, and N. Houlsby, "An image is worth 16-16 words: Transformers for image recognition at scale," in *Int. Conf. Learn. Represent.*, 2021.
- [17] D. Tabernik, S. Šela, J. Skvarč, and D. Škočaj, "Segmentation-based deep-learning approach for surface-defect detection," *J. Intell. Manuf.*, vol. 31, no. 3, pp. 759–776, 2020.
- [18] Y. Huang, C. Qiu, and K. Yuan, "Surface defect saliency of magnetic tile," *The Visual Computer*, vol. 36, no. 1, pp. 85–96, 2020.
- [19] P. Bergmann, K. Batzner, M. Fauser, D. Sattlegger, and C. Steger, "The mvtec anomaly detection dataset: a comprehensive real-world dataset for unsupervised anomaly detection," *Int. J. Comput. Vis.*, vol. 129, no. 4, pp. 1038–1059, 2021.
- [20] J. Bernal, J. Sánchez, and F. Vilarino, "Towards automatic polyp detection with a polyp appearance model," *Pattern Recognition*, vol. 45, no. 9, pp. 3166–3182, 2012.
- [21] U. Baid, S. Ghodasara, S. Mohan, M. Bilello, E. Calabrese, E. Colak, K. Farahani, J. Kalpathy-Cramer, F. C. Kitamura, S. Pati *et al.*, "The rsna-asnr-miccai brats 2021 benchmark on brain tumor segmentation and radiogenomic classification," *arXiv preprint arXiv:2107.02314*, 2021.
- [22] D.-P. Fan, T. Zhou, G.-P. Ji, Y. Zhou, G. Chen, H. Fu, J. Shen, and L. Shao, "Inf-net: Automatic covid-19 lung infection segmentation from ct images," *IEEE Trans. Med. Imag.*, vol. 39, no. 8, pp. 2626–2637, 2020.
- [23] M. Antonelli, A. Reinke, S. Bakas, K. Farahani, A. Kopp-Schneider, B. A. Landman, G. Litjens, B. Menze, O. Ronneberger, R. M. Summers *et al.*, "The medical segmentation decathlon," *Nature communications*, vol. 13, no. 1, p. 4128, 2022.